

# Dielectric Spectroscopy Can Predict the Effect of External AC Fields on the Dynamic Adsorption of Lysozyme

Tomás E. Benavidez,<sup>\*[a]</sup> José D. S. Guerra,<sup>[b]</sup> and Carlos D. Garcia<sup>\*[c]</sup>

This report describes the application of dielectric spectroscopy as a simple and fast way to guide protein adsorption experiments. Specifically, the polarization behavior of a layer of adsorbed lysozyme was investigated using a triangular-wave signal with frequencies varying from 0.5 to 2 Hz. The basic experiment, which can be performed in less than 5 min and with a single sample, not only allowed confirming the susceptibility of the selected protein towards the electric signal but also identified that this protein would respond more efficiently to signals with lower frequencies. To verify the validity of these observations, the adsorption behavior of

lysozyme onto optically transparent carbon electrodes was also investigated under the influence of an applied alternating potential. In these experiments, the applied signal was defined by a sinusoidal wave with an amplitude of 100 mV and superimposed to +800 mV (applied as a working potential) and varying the frequency in the 0.1–10000 Hz range. The experimental data showed that the greatest adsorbed amounts of lysozyme were obtained at the lowest tested frequencies (0.1–1.0 Hz), results that are in line with the corresponding dielectric features of the protein.

## Introduction

It is widely recognized that the adsorption of proteins to solid surfaces can be affected by the physicochemical properties of both the protein and the adsorbent substrate.<sup>[1–5]</sup> In addition, the adsorption process can also be modulated by external experimental conditions such as light,<sup>[6]</sup> pH, ionic strength, and temperature.<sup>[7–11]</sup> On conducting substrates, an external applied potential can also be used to control the accumulation of the protein molecules at the polarized interface.<sup>[12–18]</sup> This phenomenon is particularly important because it could open the door for the possibility to control the efficiency, selectivity, and kinetics of the adsorption process.<sup>[19]</sup> Illustrating the intriguing complexity of the adsorption process, several authors have linked the effect of the potential applied to a surface with electrostatic interactions,<sup>[20–23]</sup> orientation,<sup>[14,24,25]</sup> as well as hydration of the protein.<sup>[26]</sup> Following pioneer work by Kirkwood and Shumaker,<sup>[27]</sup> several authors have explored the possibility to affect the charge and charge distribution of proteins via external fields. This process seems to correlate with the slope of the pH titration curve<sup>[28]</sup> and that can be rationalized consider-

ing the protein's charge capacitance.<sup>[29]</sup> Along these lines, but focusing on neutral proteins and DC signals, our group reported<sup>[30]</sup> the possibility to increase the adsorbed amount of various proteins ( $\Gamma_{\text{protein}}$ ) by the influence of an external electric field ( $E_{\text{DC}}$ ). Our results demonstrated that this process was influenced by the applied potential, the structure of the protein, as well as the pH/ionic strength of the environment.<sup>[31]</sup> More importantly, they allowed us to propose that the potential applied to the selected electrode (carbon) was not only able to polarize a layer of pre-adsorbed proteins<sup>[32]</sup> but also induce the formation of a dipole in incoming protein molecules, resulting in a slow, but continuous growth of the protein film.<sup>[33]</sup> This behavior was also in agreement with molecular dynamics simulations, which suggested that the presence of the electric field was able to induce a dipolar moment in neutral proteins and increase their surface accessible solvent area (SASA), effects that contributed to their enhanced ability to interact with other proteins and further propagate the effect. At the core of these observations is the intrinsic dipolar behavior of each amino acid and each peptidic bond, conferring proteins their characteristic dielectric properties.<sup>[34]</sup> Thus, alternating electric fields have the potential to interact with the dipoles in a protein and promote conformational changes, leading to polarization.<sup>[35–38]</sup> While previous results from our group support the capacity of DC signals to induce the formation of these dipoles,<sup>[16–18,30]</sup> it is reasonable to expect that an oscillating electrical signal with frequencies in the correct range could maximize this effect and further enhance the protein adsorption process.<sup>[37,39]</sup> It is also important to state that performing adsorption experiments under precise electrochemical conditions and frequencies<sup>[40]</sup> is not a trivial task and requires not only specific instrumentation but also training in multiple areas. We believe addressing these limitations could enable other groups to select the most appropriate electrical signals to control the adsorption of proteins.

[a] Dr. T. E. Benavidez  
INFIQC-CONICET, Department of Physical Chemistry, School of Chemistry,  
National University of Córdoba, Córdoba X5000HUA, Argentina  
E-mail: tebenavidez@unc.edu.ar

[b] Prof. J. D. S. Guerra  
Institute of Physics, Federal University of Uberlândia, Uberlândia MG 38408-  
100, Brazil

[c] Prof. C. D. Garcia  
Department of Chemistry, Clemson University, Clemson SC 29634, USA  
E-mail: cdgarc@clemson.edu

© 2022 The Authors. ChemPhysChem published by Wiley-VCH GmbH.  
This is an open access article under the terms of the Creative Commons  
Attribution Non-Commercial NoDerivs License, which permits use and  
distribution in any medium, provided the original work is properly cited,  
the use is non-commercial and no modifications or adaptations are  
made.

Thus, we herein report, for the first time, the possibility to use dielectric spectroscopy to rationally select experimental conditions to control the proteins using external fields. Compared to traditional adsorption experiments, the proposed approach is simpler, faster, more robust, and only requires minimal amounts of protein. Considering its susceptibility toward the external applied potential in previous studies<sup>[30]</sup> lysozyme (LSZ) was selected as a model protein<sup>[41]</sup> and adsorbed onto carbon substrates under the influence of an oscillating potential ( $E_{AC}$ ).

## Experimental Section

### Reagents and Solutions

All aqueous solutions were prepared using 18 M $\Omega$ -cm water (NANOpure Diamond, Barnstead; Dubuque, IA) and analytical grade chemicals. Lysozyme (LSZ, from chicken egg white) was purchased from Sigma-Aldrich (St. Louis, MO). Sodium phosphate monobasic anhydrous was obtained from Fisher Scientific (Fair Lawn, NJ). AZ P4330-RS Photoresist was acquired from AZ Electronic Materials USA Corp. (Somerville, NJ). Propylene glycol monomethyl ether acetate (PGMEA 99%) was obtained from Alfa Aesar (Ward Hill, MA).

Stock solutions of LSZ (0.10 mg.mL<sup>-1</sup>) were prepared daily by dissolving a known amount of protein in 10 mmol.L<sup>-1</sup> phosphate buffer solution at pH=11.00 (IEP, isoelectric point). The latter aspect is important as this pH value avoids potential contribution of (additional) charged residues on the overall dielectric behavior of proteins.<sup>[42,43]</sup> The pH of buffer solution was adjusted using 1 mol.L<sup>-1</sup> NaOH and measured with a glass electrode connected to a digital pH meter (Orion 420A+, Thermo; Waltham, MA). Before adsorption, the protein solution was filtered through 0.2  $\mu$ m poly(tetrafluoroethylene) membrane (PTFE, VWR International; Radnor, PA) to remove any aggregates.

### Substrates

These experiments are focused on the adsorption of LSZ onto thin, optically transparent carbon films supported on silica wafers (Si/SiO<sub>2</sub>/OTCE), which were used as the conductive material to investigate the effect of the  $E_{AC}$  on the protein adsorption. As previously reported,<sup>[16]</sup> the OTCE were obtained by pyrolysis of AZ P4330-RS Photoresist. The commercial photoresist was firstly diluted to 60% v/v of the as-received material using PGMEA. Briefly, standard <111> silicon wafers (Si/SiO<sub>2</sub>, Sumco; Phoenix, AZ) were scored by a computer-controlled engraver (Gravograph IS400, Gravotech; Duluth, GA) to define pieces of 1 cm in width and 5 cm in length. The small pieces were manually cut and then cleaned using piranha solution (30% hydrogen peroxide and 70% sulfuric acid) at 90 °C for 30 min. The clean wafers were dried in a convection oven at 80 °C for 30 min. Then, a thin layer of photoresist was spread onto the silica substrates using a spin coater (Laurell, Model WS-400-6NPP; North Wales, PA). The photoresist-coated substrates were soft-baked at 110 °C for 60 s in a convection oven to evaporate the solvent and then transferred to a tube furnace (Thermolyne F21135, Barnstead International; Dubuque, IA) for pyrolysis. The carbonization procedure began by flushing the system with forming gas (95% Ar+5% H<sub>2</sub>, v/v) at 1 L.min<sup>-1</sup> for 5 min. Next, the temperature was increased at 20 °C.min<sup>-1</sup> up to 1000 °C and kept for 1 h. After pyrolysis, the samples were allowed

to cool down to room temperature, removed from the furnace, and stored in sealed glass tubes until use.

### Electrical Measurements

The response of the protein monolayer toward an applied  $E_{AC}$  can be described by its conductivity as well as polarization ( $P$ ), which refers to the separation of center of positive and negative charges in the material induced by a sufficiently-high voltage (or electric field).<sup>[44]</sup> The polarization phenomenon can be observed by measuring the displacement current that flows while the applied potential is scanned. The charge in the polarization as a function of the applied potential can be calculated, therefore, by integrating the displacement current (or in terms of the measured charges on the opposite faces on the sample), thus providing valuable information to appreciate the role of the electrical properties on the adsorption process assisted by the electric field. Because proteins do not immediately respond to the electric field, these processes are reasonable dependent on the applied frequency. Thus, to investigate the polarization behavior of LSZ, a protein monolayer was firstly adsorbed onto an OTCE at the open circuit potential (OCP, the potential at which no current flows through the cell). Following the experimental approach used for the dynamic adsorption experiments, the protein layer was obtained by immersing the OTCE in 10 mL of 0.10 mg.mL<sup>-1</sup> LSZ dissolved in 10 mmol.L<sup>-1</sup> phosphate solution at pH=11. Note that the amount of protein required to prepare individual samples can be reduced several order of magnitude (5000 times, if a volume of 50  $\mu$ L is used and vs 250 mL required for a traditional dynamic adsorption experiment). To ensure that a complete layer was obtained, the OTCE was immersed in the protein solution for at least 40 min, again following the dynamic adsorption experimental data. After drying the resulting LSZ/OTCE substrate (process that is not expected to affect the electric behavior of the proteins<sup>[42]</sup>), a thin gold layer was deposited over the protein monolayer by sputtering, to enable acquiring the electrical response of the adsorbed protein. The OTCE, as well as the sputtered gold layer, were used as the electrodes to perform the electrical measurements. These experiments were performed considering a working area of 28.3 mm<sup>2</sup>. The experimental conditions were carefully selected to minimize the possibility to denature the protein by the effect of the Joule heating. Therefore, the triangular-wave potential started at 0 mV ( $E_0$ ), increased progressively toward a positive potential ( $E_f$ ), and then returned to  $E_0$  (see Figure 1A). Depending on the experiment, the waveform frequency varied from 0.5 Hz to 2 Hz and the  $E_f$  of the triangular-wave potential modified between 410 mV and 570 mV.

The polarization ( $P$ ) was collected as a function of the applied potential by using an Agilent 33210A 10 MHz Function/Arbitrary Waveform Generator, coupled to an Agilent DSOX2004A Oscilloscope for the data collection. Next, the polarization (C.m<sup>-2</sup>) of the LSZ monolayer was calculated according to Equation 1,<sup>[44]</sup>

$$P = \frac{C_r \cdot E_f}{A} \quad (1)$$

where  $A$  represents the working area of the sample (28.3 mm<sup>2</sup>),  $E_f$  is the output voltage (potential) and  $C_r$  represents a reference capacitor, which is (conventionally) much higher than the sample's capacitance and it is used to guarantee that all the input potential by applied to the sample, thus protecting the oscilloscope from very high voltage signals. It is important to mention that each experiment takes < 5 min.

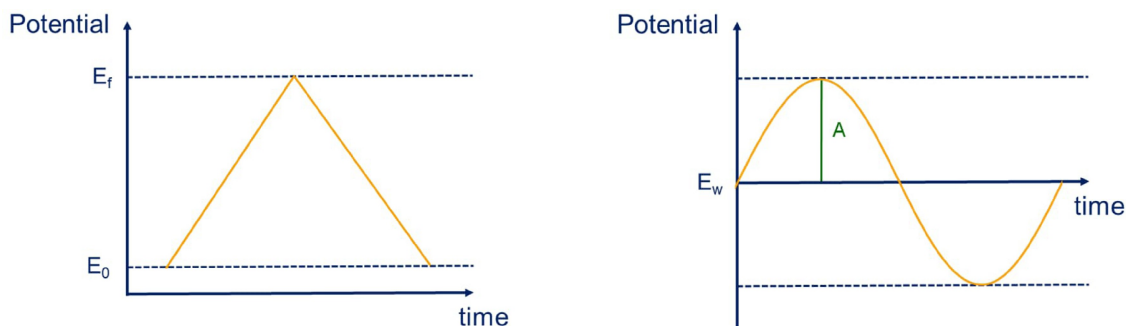


**Figure 1.** A: Schematic representation of the triangular-wave potential applied on the adsorbed monolayer to investigate the dielectric properties of LSZ. The experimental parameters were  $E_0 = 0$  mV,  $E_f = 410$ – $570$  mV, and  $f = 0.5$  Hz– $2$  Hz. B: Schematic representation of the sinusoidal potential applied on the OTCE to acquire the dynamic adsorption experiments of LSZ by ellipsometry. The electrochemical parameters were  $E_w = +800$  mV,  $A = 100$  mV, and  $f = 0.1$ – $10000$  Hz.

### Spectroscopic Ellipsometry

Adsorption experiments were carried out using a variable angle spectroscopic ellipsometer (WVASE, J.A. Woollam Co.; Lincoln, NE), following a procedure described in previous papers.<sup>[16,17,30]</sup> Briefly, SE measures the change in the reflectance and phase difference between the parallel (RP) and perpendicular (RS) components of a polarized light beam upon reflection from a surface, which are related to the amplitude ratio ( $\Psi$ ) and phase difference ( $\Delta$ ).<sup>[45,46]</sup> Experimental data were collected as a function of wavelength or time, and then modeled by using the WVASE software package (J.A. Woollam Co.; Lincoln, NE). The raw ellipsometric measurements were processed by using an optical model developed previously. The samples were described in terms of the refractive index ( $n$ ), extinction coefficient ( $k$ ), and thickness ( $d$ ). In order to describe the optical response of the sample, five uniaxial layers with optical axes parallel to the surface substrate were considered in the optical model. Accordingly, the dielectric function of Si (bulk,  $d = 1$  mm) and  $\text{SiO}_2$  ( $d = 2.1 \pm 0.5$  nm) were firstly incorporated to define the optical behavior of silica wafer. Next, the optical constants of carbon were used to explain the ellipsometric response of the OTCE ( $d = 19.6 \pm 0.7$  nm). Then, a void layer in view of nanobubbles formed on the hydrophobic and rough surface of the OTCE was also added.<sup>[47–49]</sup> The protein layer adsorbed on the OTCE was explained by a Cauchy parametrization model ( $A = 1.465$ ,  $B = 0.01$ , and  $C = 0$ ). Lastly, the optical properties of water were also taken into account because the ellipsometric experiments were acquired in aqueous solution. The mean square error (MSE, calculated by a built-in function in WVASE) was used to quantify the fitting accuracy and validate the optical model as well. In agreement with previous reports,<sup>[50,51]</sup>  $\text{MSE} < 15$  was considered acceptable.

Dynamic adsorption experiments were performed at room temperature using a modified electrochemical cell (J.A. Woollam Co.; Lincoln, NE) mounted on the vertical base of the ellipsometer, with an incident angle of  $70^\circ$ . Before the adsorption of LSZ, the thickness of the OTCE was firstly measured placing the substrate in the ellipsometry cell and performing a spectroscopic scan between 300 nm and 1000 nm (with 10 nm step) using a  $10 \text{ mmol.L}^{-1}$  phosphate buffer as the ambient medium. Then, the dynamic adsorption experiment was started by collecting a baseline on the bare OTCE at OCP, while buffer solution was injected inside the cell at a rate of  $1 \text{ mL.min}^{-1}$  using a peristaltic pump. After 20 min, the protein solution was pumped inside the cell and a LSZ monolayer was allowed to adsorb on the OTCE at the OCP. The dynamic scans always showed an initial fast process followed by a slower one during the adsorption process at OCP. This behavior was attributed to the adsorption of the protein to the bare surface, process that

has been extensively described in the literature and that is outside the scope of our studies. Following the saturation of the surface (signal reached a plateau) at open-circuit conditions, the  $E_{AC}$  with an amplitude of 100 mV was superimposed to  $+800$  mV (the working potential,  $E_w$ ) and applied and held until the end of the adsorption experiment. Note that each adsorption experiment would require approximately 25 mg of protein ( $0.1 \text{ mg.min}^{-1}$  during 240 min). As previously reported,  $E_w = +800$  mV is high enough to induce the accumulation of LSZ molecules on the OTCE without leading to electrochemical oxidation of the adsorbed proteins.<sup>[18,20,52]</sup> The  $E_{AC}$  ( $E_w = +800$  mV;  $A = 100$  mV;  $f = 0.1$ – $10000$  Hz, Figure 1BA) was applied using the impedance-time electrochemical function of a CHI660 A electrochemical analyzer (CH Instruments, Inc.; Austin, TX). The electrochemical experiments were acquired using a three-electrode configuration, where the OTCE was used as working electrode, a silver/silver chloride was used as reference electrode ( $\text{Ag}|\text{AgCl}|\text{KCl}_{\text{sat}}$ ), and a platinum wire was used as the counter electrode. After each dynamic adsorption experiment, a spectroscopic scan was always recorded to calculate the thickness of the resulting protein layer and the  $\Gamma_{\text{LSZ}}$ .

## Results and Discussion

### Electrical Response of LSZ

To understand the effect of the  $E_{AC}$  on the adsorption process, the electrical properties of the protein layer were investigated via the driving voltage dependence of polarization ( $P$ – $E$ ). In this case, a layer of LSZ was adsorbed on the OTCE (serving as one of the contacts) at the OCP and then coated with a thin layer of gold (serving as the second contact). The sample was then probed on the 0–410 mV using representative frequency values, to determine the polarization of the LSZ molecules adsorbed at the OTCE. As it can be observed in Figure 2, the polarization of the protein layer was proportional to the potential applied, leading to a plateau in the polarization that was dependent on the frequency applied. In the specific case of the experiment performed at the lowest frequency studied (0.5 Hz), the polarization was stabilized ( $3.74 \text{ C.m}^{-2}$ ) at approximately 250 mV. This dependence of the polarization with respect to the applied potential has been reported for other systems<sup>[12,32]</sup> and is somewhat consistent with dynamic adsorption experiments previously reported.<sup>[18]</sup> Indeed, different to the  $P$ – $E$  curve

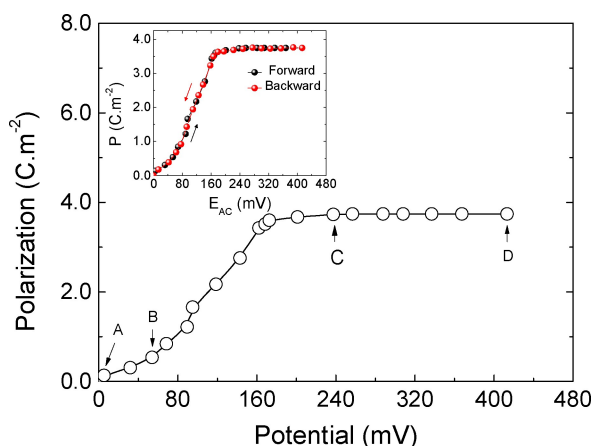


**Figure 2.** Effect of the triangular-wave potential ( $E_{AC}$ ) on the polarization of an adsorbed monolayer of LSZ located between an OTCE and a thin gold layer, performed at 0.5 Hz. Figure inset shows the forward and backward pathways of the polarization with the increasing and decreasing voltage, respectively.

expected for linear dielectrics, an evident non-linear behavior was observed, which can be ascribed to the strong electric field (or voltage, noting that  $E=V/h$  being  $h$  the sample's thickness) dependence of the electrical susceptibility of the material and evidencing the influence of the external driving potential on the material's dipoles rearrangement.<sup>[53]</sup> That is, the observed non-linear variation is ascribed to the phase difference between the driving potential intensity and polarization promoted by the different rates at which the dipoles and the potential change. At the macroscopic level, for instance, an applied voltage leads to a shift in the spatial distribution of bound charges, identified as polar groups in organic compounds (polar protein molecules, in the present case), which is quantified as polarization.<sup>[44,54]</sup>

As it can be also observed in Figure 2, the initial poling process involves a gradual transition of dipole arrangement and formation. Once poled, the polarization dependence on applied potential becomes linear as neighboring dipoles aligned to the driving potential have grown to promote the formation of the polar groups. At low driving voltage values, the polarization increases linearly with the potential amplitude, according to relation  $P=\chi E^{[44,53]}$  being  $\chi$  the material's electrical susceptibility and  $E$  the external electric field (or potential). That is, polar groups pattern remains unchanged, and the ions are only shifted within the neighborhood of their equilibrium positions. Therefore, a linear behavior between  $P$  and  $E$  is achieved (A–B segment). In this linear region, the field is not strong enough to reorient dipolar species with unfavorable polarization direction; that is, with polarization orientation different to the field direction. As the field is increased, the polarization of polar groups with unfavorable direction of polarization will start to reorient to a more energetically favorable direction (as close as possible to the direction of the field), thus rapidly increasing the measured charge density (non-linear intermediate B–C segment). In this region, a number of polar groups with a polarization misaligned with the field direction will start to

reorient along the field direction and macroscopic polarization will increase rapidly until the saturation is attained (above-mentioned plateau in the polarization), where all the dipolar species are aligned with the electric field direction. In other words, when all the polar regions have become oriented parallel to the external field, the polarization reaches a saturation level (C–D segment) and it is called saturation polarization ( $P_s$ ). It is worth noting that, by reducing back the electric field strength, the polarization will decrease again until reach the initial zero-polarization state, thus returning back to the starting value. This behavior can be better observed in the inset of Figure 2, which depicts the effect of forward and backward applied voltage on the polarization. While the applied potentials in both experiments cannot be directly compared, these results support the hypothesis that the driving potential applied to the surface can enhance the adsorption process via electrical polarization and that such effect would be dependent on the potential strength.<sup>[16–18,30]</sup>

To obtain more information about the effect of the triangular-wave potential, the polarization of the LSZ layer was also investigated as a function of the frequency of the applied voltage. In order to match the proposed experimental design (*vide infra*, Figure 5 and Table 1), experiments were performed in the 0–410 mV range and using 0.5 Hz, 1.0 Hz, and 2.0 Hz. Representative results are shown in Figure 3. As can be observed, the polarization of the protein layer was significantly dependent on the frequency of the oscillating driving voltage, affecting not only the maximum polarization of LSZ layer but also the potential required to reach the inflection point. In agreement with the dynamic adsorption experiments, the lower the frequency of the alternating electric field the higher the effect on the adsorption process, effect that was related to the polarizability of the protein layer. It is important to point out that no hysteresis response was observed for all the applied frequencies, suggesting that the polarization of the protein layer could be considered a reversible process under the investigated experimental conditions. From the fundamental point of view, the notable decreases in the macroscopic polarization with the increase of the frequency, reflects the dynamics of the dipolar groups' reorientation under applied alternate electric field, and has been ascribed in non-linear dielectrics to the systematic dielectric loss of reorientable polarization under repetitive cycling voltage amplitude.<sup>[55]</sup> This

**Table 1.** Initial adsorption rate (calculated after the corresponding potential was applied,  $d\Gamma/dt_1$ ), linear approximation of the second adsorption process ( $d\Gamma/dt_2$ , calculated in the 150–240 min interval of the experiment) and final adsorbed amount of LSZ under AC stimulation ( $E_w = +800$  mV,  $A = 100$  mV) onto LSZ/OTCE substrate as a function of frequency.

Frequency [Hz]	$d\Gamma/dt_1$ [ $\times 10^{-2}$ mg.m <sup>-2</sup> .min <sup>-1</sup> ]	$d\Gamma/dt_2$ [ $\times 10^{-2}$ mg.m <sup>-2</sup> .min <sup>-1</sup> ]	$\Gamma@240$ min [mg.m <sup>-2</sup> ]
$E_{DC}$	51 ± 2	3.039 ± 0.004	7.3 ± 0.2
0.1	91 ± 7	9.044 ± 0.008	13.7 ± 0.3
0.5	78 ± 6	9.512 ± 0.006	14.0 ± 0.4
1	101 ± 9	8.320 ± 0.003	14.2 ± 0.3
10	70 ± 6	5.527 ± 0.004	10.2 ± 0.2
100	77 ± 6	5.064 ± 0.004	10.4 ± 0.2
10000	65 ± 4	5.181 ± 0.003	9.2 ± 0.2

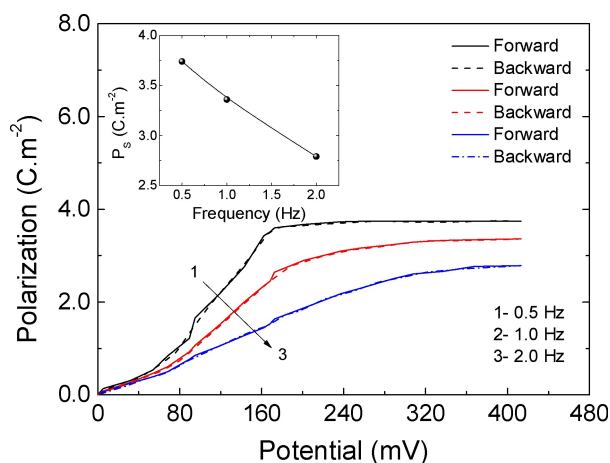


**Figure 3.** Frequency dependence of the polarization versus applied potential response, for the same adsorbed monolayer of LSZ located between an OTCE and a thin gold layer. Figure inset shows the frequency dependence of the saturation polarization ( $P_s$ ).

is the well-known fatigue effect, which in most of the cases (including bulk, thin films and polymeric compounds) has been related to the electrode-material interface effects.<sup>[56,57]</sup> In fact, the injection of charges at the interface could promote structural defects (space charge or charged point defects),<sup>[58–60]</sup> which act as pinning center for the dipoles reorientation thus resulting in a reduced polarization and increasing the fatigue rate.

The effect of successive potentials applied to the triangular-wave ( $E_f$ ) on the polarization of the LSZ monolayer was also evaluated at 0.5 Hz (as it provides the maximum response), using 410 mV, 450 mV, 500 mV, and 570 mV. Results, shown in Figure 4A, revealed a gradual decrease in the polarization of the LSZ as the applied potential was increased, which can be better observed in Figure 4B, for the maximum polarization ( $P_m$ ) reached at each maximum applied voltage ( $E_m$ ). These observed

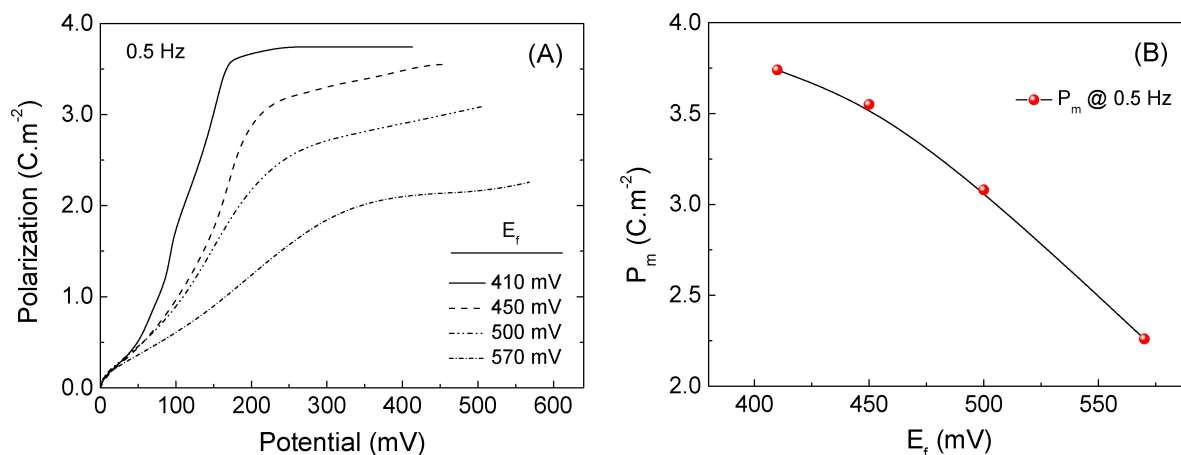


**Figure 4.** (A) Effect of the successive increasing potential on the polarization of an adsorbed monolayer of LSZ placed between an OTCE and a gold layer. The frequency was set at 0.5 Hz. (B) Performance of the maximum polarization ( $P_m$ ) of a LSZ monolayer on account of the successive increasing  $E_f$  potentials at a frequency of 0.5 Hz.

changes on the polarization response were attributed to an aging-like effect of the polarization, induced by the inclusion of point defects after each voltage cycle. Such structural defects could act as trapping centers for the dipoles' reorientation under applied potential. On the other hand, as also noted previously, the polarization process showed to be also reversible for each of the selected potential values (data not shown).

### Effect of the Oscillating Field on the Adsorption of LSZ

To demonstrate the possibility to transfer the knowledge from dielectric spectroscopy to the experiments performed in solution, dynamic adsorption experiments were carried out at room temperature by modifying the frequency of the alternating sinusoidal potential within the 0.1–10000 Hz range. For all adsorption experiments, a potential wave with a fixed amplitude of 100 mV was superimposed to a constant working potential ( $E_w = +800$  mV). Every dynamic adsorption experiment started by recording a baseline while the buffer solution (10 mmol.L<sup>-1</sup> phosphate buffer at pH=11) was pumped into the electrochemical cell at 1 mL.min<sup>-1</sup> and no potential was applied on the OTCE surface. After 20 min, a solution containing 0.10 mg.mL<sup>-1</sup> LSZ dissolved in phosphate solution at pH=11 was injected to allow a protein monolayer to adsorb onto the electrode at the OCP. According to the adsorption behavior of structure-stable proteins, it is reasonable to consider that minimum structural rearrangements would be displayed by the LSZ molecules upon the interaction with the OTCE surface.<sup>[61]</sup> Considering the molecular dimensions of LSZ (4.5 nm × 3.0 nm × 3.0 nm),<sup>[62]</sup> the thickness of the protein layer (3.9 ± 0.5 nm, N = 9) achieved at OCP suggest the formation of a layer of adsorbed proteins on the OTCE (see t = 60 min, Figure 5). Although the data obtained does not allow drawing conclusions about the surface coverage or orientation of the proteins on the surface, the thickness obtained suggests a (random) arrangement of proteins with a mix of head-on and side-on orientations. As a

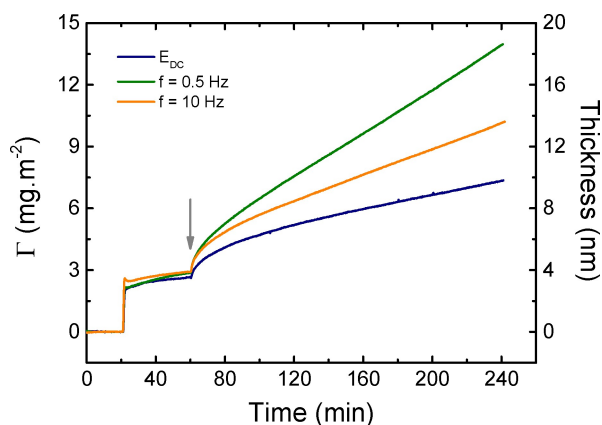


**Figure 5.** Effect of the frequency of the applied  $E_{AC}$  with an amplitude of 100 mV and superimposed at  $E_{DC} = +800$  mV on the adsorption kinetic of  $0.10 \text{ mg}\cdot\text{mL}^{-1}$  LSZ after adsorbing a protein monolayer on the OTCE at OCP. The arrow shows the moment when the potential was applied.

reference, the latter possibility would yield a maximum thickness of 3 nm (at full coverage). After the surface was saturated (and a plateau in the signal was obtained), the  $E_{AC}$  was applied and kept until the end of every adsorption experiment, typically  $t = 240$  min. As a control experiment, that highlights the effects displayed by the  $E_{AC}$ , a dynamic adsorption experiment applying a constant potential ( $E_{DC} = +800$  mV) was also carried out. Representative results for the dynamic adsorption experiments are shown in Figure 5.

As reported elsewhere,<sup>[16,17,30]</sup> a rapid accumulation of LSZ was observed immediately after the potential was applied. The process is analyzed in terms of a fast initial process ( $d\Gamma/dt_1$ ) that transitioned into a secondary, much slower process ( $d\Gamma/dt_2$ ), approximated to a first-order reaction, and that allowed the accumulation of significantly larger amounts of protein on the surface, again with respect to results obtained under OCP conditions. It is important to reiterate that these processes were attributed to the polarization of the proteins in the vicinity of the electrode surface and cannot be attributed to traditional electrostatic (experiments performed at the corresponding IEP) or hydrophobic interactions (equilibrated upon the formation of the first layer of protein).<sup>[30]</sup> Figure 5 also shows that the secondary adsorption process was strongly dependent on the frequency applied. Specifically, our experimental results, summarized in Table 1, demonstrated that the  $E_{AC}$  (at any of the investigated frequencies) was able to exert a much stronger effect on the accumulation of LSZ molecules onto the electrode (when compared to the adsorption promoted by the  $E_{DC}$ ). Although all selected  $E_{AC}$  increased the  $\Gamma_{LSZ}$  (vs.  $E_{DC}$ ), the highest amounts of LSZ were observed when the alternating electric field switched slowly, around 0.5 Hz and 1 Hz.

To understand the adsorption of LSZ, some issues referred to the experimental conditions had to be considered. On one side, a protein layer was always adsorbed at the OCP so the polarization of the protein layer by the electric field was contemplated. The other concern to keep in mind was how the polarized layer promoted the adsorption of the LSZ molecules

in aqueous phase. Based on the experimental data and the characteristic structural stability of LSZ, it is reasonable to assume that the alignment of the protein inner dipoles would require more time (lower frequencies). This observation is in line with previous reports,<sup>[38,39]</sup> stating that the polarization of proteins does not instantly follow the electric field. That delay has been attributed to the dielectric relaxation of the protein molecules inducing an energy loss.<sup>[63]</sup> In this regard, the dielectric relaxation increased at the highest frequencies and consequently the adsorbed amount of LSZ decreased as demonstrated the dynamic adsorption experiments. It is also important to mention that our results are somewhat different from those reported by Htwe *et al.*<sup>[21]</sup> who reported the adsorption of LSZ to various metals and that attributed the effect to a combination of electric force and electrostatic interactions with ionized surface hydroxyl groups. Other groups have also pointed to the importance of counterions at the surface of the electrode.<sup>[64]</sup>

## Conclusions

In this work, the electrical properties of a protein monolayer were preliminarily screened using dielectric spectroscopy (following the polarization response). Although a detailed characterization of the process was obtained, the basic information could be obtained with a single sample and in less than 5 min. According to our results, a significant increment of the polarization of the LSZ monolayer was observed when lower frequency decreased, leading to a memory effect on the protein monolayer polarization. This special feature was considered the root of the differences observed in the adsorption experiments. Following these results, the adsorption of LSZ was then investigated by as a function of the frequency applied, revealing that the adsorption of LSZ was significantly increased by the influence of the alternating potential. More importantly, the adsorption of LSZ increased when the frequency of the  $E_{AC}$  decreased, in line with the behavior observed in the solid electrodes. The results showed that the polarization of the LSZ monolayer played a decisive role on the protein adsorption and can be reasonably anticipated by electrical measurements. Although the experimental data contributed successfully to explain the dynamic adsorption behavior of LSZ, the influence of the  $E_{AC}$  should be extended to a larger number of proteins (e.g. "hard" vs. "soft" proteins) to acquire a more general idea about how the (di)electric properties of the proteins could be used to modulate their adsorption behavior.

## Acknowledgements

Financial support for the project has been provided by the National Scientific and Technological Research Council (CONICET) from Argentina, the Physicochemical Research Institute of Córdoba (INFIQC), Department of Physical Chemistry, School of Chemistry, National University of Córdoba, Clemson University, the National Council of Scientific and Technological Development

(CNPq) grant 303447/2019-2, Minas Gerais Research Foundation (FAPEMIG) grants PPM-00661-16 and APQ-02875-18 and Coordenação de Aperfeiçoamento de Pessoal de Nível Superior – Brasil (CAPES) – Finance Code 001.

## Conflict of Interest

The authors have no competing interests to declare that are relevant to the content of this article.

## Data Availability Statement

The data that support the findings of this study are available from the corresponding author upon reasonable request.

**Keywords:** lysozyme · adsorption · dielectric spectroscopy · carbon · AC fields

- [1] W. Norde, *Macromol. Symp.* **1996**, *103*, 5–18.
- [2] A. W. Vermeer, W. Norde, *J. Colloid Interface Sci.* **2000**, *225*, 394–397.
- [3] W. Norde, C. E. Giacomelli, *J. Biotechnol.* **2000**, *79*, 259–268.
- [4] A. M. Puziy, O. I. Poddubnaya, A. Derylo-Marczewska, A. W. Marczewski, M. Blachnio, M. M. Tsyba, V. I. Sapsay, D. O. Klymchuk, *Adsorption*. **2016**, *22*, 541–552.
- [5] M. Rabe, D. Verdes, M. Rankl, G. R. J. Artus, S. Seeger, *ChemPhysChem*. **2007**, *8*, 862–872.
- [6] J. Zhang, T. Hu, Y. Liu, Y. Ma, J. Dong, L. Xu, Y. Zheng, H. Yang, G. Wang, *ChemPhysChem* **2012**, *13*, 2671–2675.
- [7] E. A. Vogler, *Biomaterials*. **2012**, *33*, 1201–1237.
- [8] W. Norde, *Colloids and Interfaces in Life Sciences and Bionanotechnology*, CRC Press, **2011**.
- [9] W. Norde, *Colloids Surf. B*. **2008**, *61*, 1–9.
- [10] M. Rabe, D. Verdes, S. Seeger, *Adv. Colloid Interface Sci.* **2011**, *162*, 87–106.
- [11] M. d. S. Gama, A. G. Barreto, F. W. Tavares, *Adsorption*. **2021**, *27*, 1137–1148.
- [12] J. G. Fraaije, J. M. Kleijn, M. van der Graaf, J. C. Dijt, *Biophys. J.* **1990**, *57*, 965–975.
- [13] P. Bernabeu, A. Caprani, *Biomaterials*. **1990**, *11*, 258–264.
- [14] M. A. Brusatori, Y. Tie, P. R. Van Tassel, *Langmuir*. **2003**, *19*, 5089–5097.
- [15] Y. Y. Song, Y. Li, C. Yang, X. H. Xia, *Anal. Bioanal. Chem.* **2008**, *390*, 333–341.
- [16] T. E. Benavidez, C. D. Garcia, *Electrophoresis*. **2013**, *34*, 1998–2006.
- [17] T. E. Benavidez, C. D. Garcia, *Langmuir*. **2013**, *29*, 14154–14162.
- [18] T. E. Benavidez, D. Torrente, M. Marucho, C. D. Garcia, *J. Colloid Interface Sci.* **2014**, *435*, 164–170.
- [19] P. A. Fritz, B. Bera, J. van den Berg, I. Visser, J. M. Kleijn, R. M. Boom, C. G. P. H. Schroën, *Langmuir*. **2021**, *37*, 6549–6555.
- [20] V. Brabec, I. Schindlerová, *J. Electroanal. Chem. Interfacial Electrochem.* **1981**, *128*, 451–458.
- [21] H. Ei Ei, Y. Nakama, H. Tanaka, H. Imanaka, N. Ishida, K. Imamura, *Colloids Surf. B*. **2016**, *147*, 9–16.
- [22] E. E. Htwe, Y. Nakama, Y. Yamamoto, H. Tanaka, H. Imanaka, N. Ishida, K. Imamura, *Colloids Surf. B*. **2018**, *166*, 262–268.
- [23] J. G. Wu, S. C. Wei, S. C. Luo, *Adv. Mater. Interfaces*. **2020**, *7*, 2000470.
- [24] M. Rabe, D. Verdes, S. Seeger, *Adv. Colloid Interface Sci.* **2011**, *162*, 87–106.
- [25] C. D. Cooper, N. C. Clementi, L. A. Barba, *J. Chem. Phys.* **2015**, *143*, 124709.
- [26] P. A. Fritz, B. Bera, J. van den Berg, I. Visser, J. M. Kleijn, R. M. Boom, C. Schroën, *Langmuir*. **2021**, *37*, 6549–6555.
- [27] J. G. Kirkwood, J. B. Shumaker, *Proc. Natl. Acad. Sci. USA* **1952**, *38*, 863.
- [28] M. Lund, T. Akesson, B. Jonsson, *Langmuir*. **2005**, *21*, 8385–8388.
- [29] M. Lund, B. Jonsson, *Biochem.* **2005**, *44*, 5722–5727.
- [30] T. E. Benavidez, D. Torrente, M. Marucho, C. D. Garcia, *Langmuir*. **2015**, *31*, 2455–2462.
- [31] P. R. Van Tassel, *Curr. Opin. Colloid Interface Sci.* **2012**, *17*, 106–113.
- [32] A. Koutsoubas, D. Lairez, G. Zalczer, F. Cousin, *Soft Matter*. **2012**, *8*, 2638–2643.
- [33] P. Van Tassel, in *Proteins at Solid-Liquid Interfaces. Principles and Practice. Vol* (Eds.: P. Dejardin) Springer, **2006**, pp. 1–22.
- [34] R. Pethig, *IEEE Trans. Electr. Insul.* **1984**, *El-19*, 453–474.
- [35] A. Bonincontro, A. De Francesco, G. Onori, *Colloids Surf. B*. **1998**, *12*, 1–5.
- [36] C. Cametti, S. Marchetti, C. M. Gambi, G. Onori, *J. Phys. Chem. B*. **2011**, *115*, 7144–7153.
- [37] I. Bekard, D. E. Dunstan, *Soft Matter*. **2014**, *10*, 431–437.
- [38] K. Deshmukh, S. Sankaran, B. Ahamed, K. K. Sadasivuni, K. S. K. Pasha, D. Ponnamma, P. S. Rama Sreekanth, K. Chidambaram, in *Dielectric Spectroscopy, Vol.* (Eds.: S. Thomas, R. Thomas, A. K. Zachariah, R. K. Mishra), Elsevier, **2017**, pp. 237–299.
- [39] F. Bibi, M. Villain, C. Guillaume, B. Sorli, N. Gontard, *Sensors*. **2016**, *16*.
- [40] A. Budi, F. S. Legge, H. Treutlein, I. Yarovsky, *J. Phys. Chem. B*. **2005**, *109*, 22641–22648.
- [41] K. C. D. S. Figueiredo, V. M. M. Salim, T. L. M. Alves, J. C. Pinto, *Adsorption*. **2005**, *11*, 131–138.
- [42] J. W. Pitera, M. Falta, W. F. van Gunsteren, *Biophys. J.* **2001**, *80*, 2546–2555.
- [43] M. Amin, J. Kupper, *ChemistryOpen*. **2020**, *9*, 691–694.
- [44] C. J. F. Böttcher, *Theory of Electric Polarization*, Elsevier, Amsterdam, **1973**.
- [45] H. Fujiwara, *Spectroscopic Ellipsometry: Principles and Applications*, Wiley, **2007**.
- [46] M. Canepa, in *A Surface Scientist's View on Spectroscopic Ellipsometry, Vol.* (Eds.: G. Bracco, B. Holst), Springer Berlin Heidelberg, Berlin, Heidelberg, **2013**, pp. 99–135.
- [47] W. Zhou, J. Niu, W. Xiao, L. Ou, *Ultrason. Sonochem.* **2019**, *51*, 31–39.
- [48] J. W. Tyrrell, P. Attard, *Phys. Rev. Lett.* **2001**, *87*, 176104.
- [49] J. W. G. Tyrrell, P. Attard, *Langmuir*. **2002**, *18*, 160–167.
- [50] M. F. Mora, M. R. Nejadnik, J. L. Baylon-Cardiel, C. E. Giacomelli, C. D. Garcia, *J. Colloid Interface Sci.* **2010**, *346*, 208–215.
- [51] M. R. Nejadnik, F. L. Deepak, C. D. Garcia, *Electroanalysis*. **2011**, *23*, 1462–1469.
- [52] T. E. Benavidez, M. E. Wechsler, M. M. Farrer, R. Bizios, C. D. Garcia, *Tissue Eng. Part C Methods*. **2016**, *22*, 69–75.
- [53] C. Kittel, *Introduction to Solid State Physics*, New York-London **1971**.
- [54] I. S. Zheludev, *Physics of Crystalline Dielectrics: Volume 2 Electrical Properties*, Springer US, **1971**.
- [55] A. K. Tagantsev, I. Stolichnov, E. L. Colla, N. Setter, *J. Appl. Phys.* **2001**, *90*, 1387–1402.
- [56] Q. Jiang, W. Cao, L. E. Cross, *J. Am. Ceram. Soc.* **1994**, *77*, 211–215.
- [57] X. J. Lou, *J. Appl. Phys.* **2009**, *105*, 024101.
- [58] X. Du, I. W. Chen, *J. Appl. Phys.* **1998**, *83*, 7789–7798.
- [59] F. Yan, P. Bao, H. L. W. Chan, C.-L. Choy, Y. Wang, *Thin Solid Films* **2002**, *406*, 282–285.
- [60] Y. Wang, K. F. Wang, C. Zhu, T. Wei, J. S. Zhu, J. M. Liu, *J. Appl. Phys.* **2007**, *101*, 046104.
- [61] M. M. Ouberai, K. Xu, M. E. Welland, *Biomaterials* **2014**, *35*, 6157–6163.
- [62] M. A. Bos, Z. Shervani, A. C. I. Anusiem, M. Giesbers, W. Norde, J. M. Kleijn, *Colloids Surf. B*. **1994**, *3*, 91–100.
- [63] M. Wolf, R. Gulich, P. Lunkenheimer, A. Loidl, *Biochim. Biophys. Acta* **2012**, *1824*, 723–730.
- [64] Y. Xie, C. Liao, J. Zhou, *Biophys. Chem.* **2013**, *179*, 26–34.

Manuscript received: January 3, 2022  
 Revised manuscript received: February 25, 2022  
 Accepted manuscript online: February 28, 2022  
 Version of record online: March 23, 2022